NANO LETTERS

2008
Vol. 8, No. 9
2632-2637

Enhanced Fluid Flow through Nanoscale Carbon Pipes

Max Whitby,[†] Laurent Cagnon,[‡] Maya Thanou,[†] and Nick Quirke*[,†]

Chemistry Department, Imperial College, South Kensington, London SW7 2AZ, United Kingdom, and Institut Néel, CNRS et Université Joseph Fourier, BP 166, F-38042 Grenoble Cedex 9, France

Received March 10, 2008; Revised Manuscript Received June 3, 2008

ABSTRACT

Recent experimental and theoretical studies demonstrate that pressure driven flow of fluids through nanoscale (d < 10 nm) carbon pores occurs 4 to 5 orders of magnitude faster than predicted by extrapolation from conventional theory. Here, we report experimental results for flow of water, ethanol, and decane through carbon nanopipes with larger inner diameters (43 ± 3 nm) than previously investigated. We find enhanced transport up to 45 times theoretical predictions. In contrast to previous work, in our systems, decane flows faster than water. These nanopipes were composed of amorphous carbon deposited from ethylene vapor in alumina templates using a single step fabrication process.

The behavior of fluids flowing through nanoscale channels is an active focus of current research.[1] Novel transport phenomena including dramatically enhanced flows have been discovered, with far-reaching implications for our theoretical understanding of the dynamics of fluids highly confined in one or two dimensions. Useful practical applications for nanofluidic technologies in medicine and in process engineering have been proposed to exploit these emerging physical properties.[2–4] There is particular interest in carbon as a potentially biocompatible nanomaterial from which such nanofluidic devices can readily be fabricated.[5,6]

The present study extends experimental investigation of enhanced nanofluidic flow to previously unreported materials (templated amorphous carbon nanopipes) and to a new scale (~50 nm diameter pores). Two recent experimental studies have previously demonstrated unexpectedly rapid transport of fluids through the smaller central pores of carbon nanotubes. Writing in *Nature*, Majumder et al. reported an average velocity for water flowing through 7 nm pores in an aligned sealed array of multiwalled carbon nanotubes (MWNT) more than 60 000 times greater than predicted using conventional fluid flow theory.[7] For ethanol, they reported an enhancement factor ~32 000 times and for decane ~4000 times. They attributed increased fluid velocities to an essentially frictionless interface at the carbon nanotube inner wall. The following year in 2006, Holt et al. writing in *Science* reported minimum flow enhancements in the range 560 to 8400 for water through even smaller 1−2 nm diameter pores in an aligned array of double-walled carbon nanotubes sealed in a silicon nitride matrix.[8] These findings, along with the results from several relevant simulation studies,[9–11] prompted a recent theoretical investigation into the phenomenon by Joseph et al.,[12] including a molecular dynamics (MD) study of fast water transport in carbon nanotubes. The authors attributed the enhanced flow to a velocity jump in a depletion layer at the interface between the nanotube wall and the water molecules. They further argued that the formation of a hydrogen bonding network, strongly influenced by surface roughness and the state of chemical functionalization of the carbon wall, plays a significant role in determining flow.

The above-mentioned studies all consider fluid flow through sub-10 nm graphitic channels comprised of the central cores of carbon nanotubes with a nested fullerene molecular structure. Earlier experimental investigations indicated the possibility of flow enhancement for *n*-propanol through much larger 800 nm silicon channels[13] and separately for decane, hexadecane, and silicone oil through sub-200 nm channels in a polymeric photoresist.[14] The extent of departure from conventionally predicted flow was modest (much less than an order of magnitude) and no enhancement was observed for water through these materials even down to a channel width of 40 nm.

A gap therefore existed in our knowledge of nanoscale fluid flow, particularly for the scale regime between 10 nm and 100 nm and specifically for channels composed of carbon in which such dramatic flow enhancement through nanotubes has recently been found. Thus, the aim of the experimental investigation reported here is to determine the extent to which fluid transport is enhanced for flow through larger (though still nanoscale) carbon channels. Furthermore, the form of

* Corresponding author. E-mail: n.quirke@imperial.ac.uk. Phone: +44 (0)20 7594 5844. Fax: +44 (0)20 7594 5850.
† Chemistry Department, Imperial College.
‡ Institut Néel, CNRS et Université Joseph Fourier.

10.1021/nl080705f CCC: $40.75
Published on Web 08/05/2008

carbon nanopipe investigated in these experiments is different from carbon nanotubes. We studied carbon nanopipes composed of a layer of amorphous carbon built up on the porous surfaces of an anodic aluminum oxide (AAO) template using chemical vapor deposition (CVD). This templated method of producing carbon nanopipes is in contrast to the more widely known vapor−liquid−solid (VLS) growth of carbon nanotubes from nanoscale metal particle catalysts. The use of AAO templates to produce carbon nanopipes via CVD was first described in 1998[15] and the technique arose from a more general interest in templated synthesis of nanomaterials.[16]

Templated carbon nanopipes have a number of features that make them attractive for fabrication of nanofluidic devices including a larger open inner pore relative to the outer diameter, ready dimensional control through selection of the AAO template, wall-thickness control by varying CVD time, and straightforward patterning into well-ordered, highly aligned and dense arrays. Importantly for the accurate measurement of pressure driven flow, the intact as-produced nanopipe arrays are embedded in the parent AAO matrix thus forming a robust composite which can act as a membrane. Furthermore, production can be achieved in a single step using CVD, with a regular, high density array of pores lined with a continuous layer of pure carbon. This provides a straightforward and easily achievable means of ensuring that fluid is transported exclusively along the central inner pores and not through possible gaps existing between the outer carbon nanopipe walls. In contrast, preparation of the MWNT and DWNT membrane arrays deployed in the previous experimental studies has involved elaborate gap-filling, pore-opening, and plasma-etching steps.[7,8] This has required sophisticated equipment typically employed in the fabrication of semiconductor devices.

A severe difficulty previously hindering production of simple templated carbon nanopipe arrays in a form suitable for studying nanoscale fluid transport (ie through pores <100 nm) has been the unavailability of high quality AAO templates with satisfactory pore morphology. In initial experiments, several commercially available templates with nominally suitable pore diameters were obtained and characterized using scanning electron microscopy (SEM) and atomic force microscopy (AFM). Isolated single carbon nanopipes produced by CVD inside such templates were also imaged by transmission electron microscopy (TEM) following etching away of the surrounding alumina matrix with dilute alkali solution. All three characterization methods revealed that carbon nanopipe arrays grown in commercially available templates with pore diameters of 100 nm and below were unsuitable for use in pressure driven flow experiments because of irregular morphology. Stated inner diameters often applied only to the final few micrometers of much longer (typically 50 μm), wider (typically >200 nm) channels. Pore shape on one side of the resulting membranes was often highly variable, with a wide distribution of aperture sizes and a strong tendency to provoke pore blocking during CVD. See Supporting Information for characterization data.

To overcome this obstacle, we carefully prepared our own AAO templates to ensure regularly spaced pores of uniform <100 nm inner diameter along their entire length. Template production was based on methods previously described in the literature.[17,18] See Supporting Information. In brief, high purity aluminum plates were mechanically polished until a mirror-like finish was obtained. This was followed by electropolishing. Then, a two-step anodizing procedure in 0.5 M oxalic acid at 40 V was used to obtain the template. This was followed by removal of the aluminum substrate and, finally, a pore opening and widening treatment. The membranes thus obtained showed well-ordered arrays of pores with diameter of 62 ± 4 nm and distance between pore centers of 102 ± 1 nm and thickness of 78 ± 2 μm. See Figure 1a,c and also Supporting Information for further details.

The carbon nanopipes for transporting fluids were grown inside these templates by CVD using a variation on previously published methods.[19] In brief, the templates were first cut to size ($\sim 9 \times 9$ mm) with a scalpel and annealed at 675 °C for 4 h between quartz plates to prevent curling during subsequent CVD. Slow ramping up to and down from the annealing temperature was critical for success of this step. A mixture of 30% ethylene and 70% helium (Scott Specialty Gases, premixed) was flowed at 60 sccm for 2 h over the templates once their temperature was stable at 675 ± 3 °C. They were supported using tungsten wires in a ceramic boat with the axis of their pores perpendicular to the direction of gas flow. Heating and cooling occurred at the natural ramp of the tube furnace (Vecstar with 25 mm quartz tube) in a 100 sccm stream of argon (Pureshield 99.995%, British Oxygen Company).

The resulting carbon nanomembranes were examined using optical microscopy at a magnification of 100×, and any showing indications of cracking or other gross defects were discarded. SEM (LEO 1525 Gemini with field emission gun) was used to confirm that the pores remained open, to assess evenness of carbon deposition, and to obtain calibrated micrographs from which average pore diameter was determined to be 43 ± 3 nm. SEM was also used to confirm nanopipe uniformity by examining a snapped fragment on its side in cross section. See Figure 1b,c,d. Another fragment was sonicated at low power (Jencons cleaning bath) for 30 min in 2 N NaOH aqueous solution followed by triple washing in deionized water with centrifugation at 13 000 rpm. This procedure completely etched away the alumina template matrix, leaving behind intact nanopipes. A suspension of these carbon pipes was allowed to dry on a 300 mesh holey carbon film grid and was examined using TEM (Jeol FX2000) to assess nanopipe wall thickness and uniformity. See Figure 2. The average inner diameter of the pores was measured from the TEM micrographs to be 46 ± 3 nm, and the carbon wall thickness was measured to be 6 ± 1 nm. This value is in good agreement with the figure obtained from the SEM characterization.

To measure fluid flow through the nanopipes, it was first necessary to mount each approximately square membrane fragment in a specially manufactured circular brass adapter

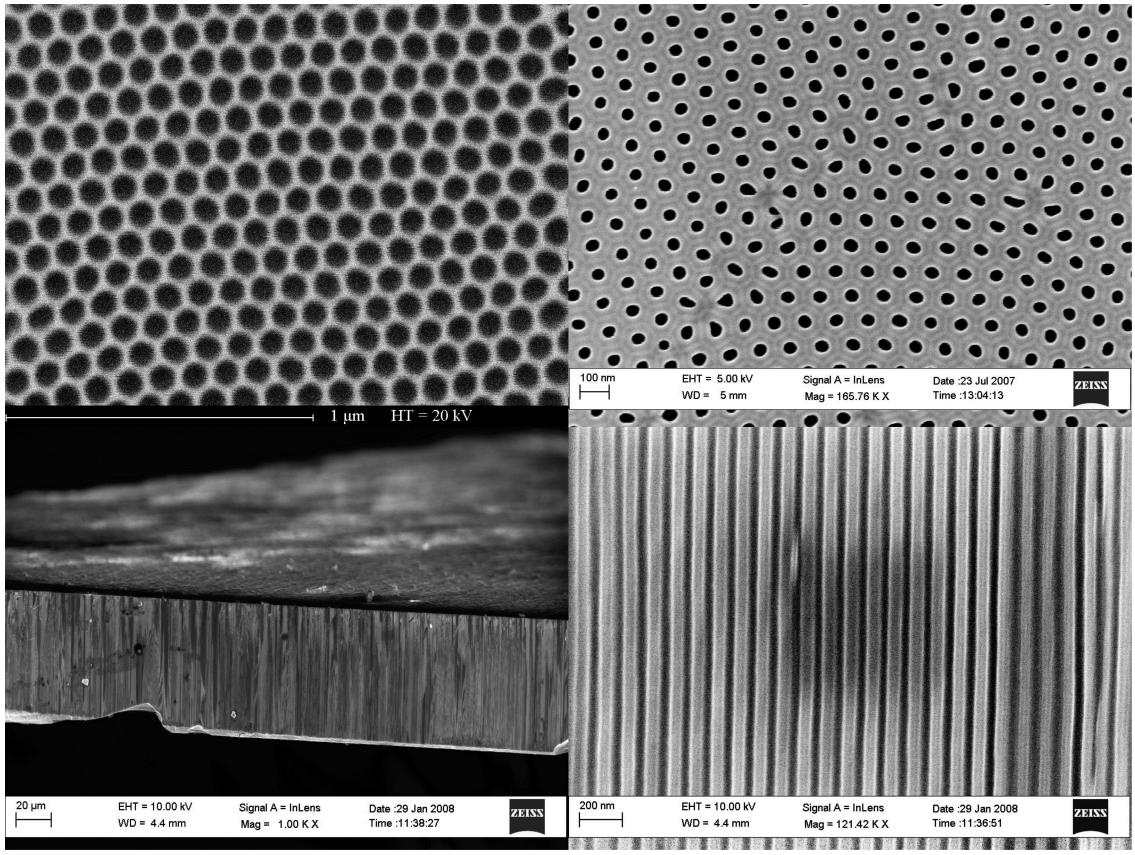

Figure 1. SEM images showing (a; top left) surface of porous alumina template prior to CVD treatment; (b; top right) template after CVD now covered in a layer of amorphous carbon which has reduced the diameter of the pores; (c; bottom left) cross section through snapped membrane; (d; bottom right) higher magnification view of cross section revealing the well-aligned and highly regular carbon nanopipe array.

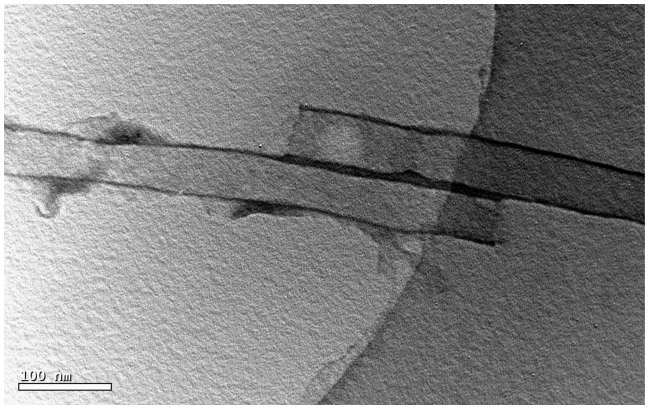

Figure 2. TEM image of two amorphous carbon nanopipes isolated from the AAO template showing an average inner channel diameter of 46 ± 3 nm. The darker region on the right third of the frame is the carbon film from the TEM grid supporting the sample.

compatible with standard commercially available stainless steel 13 mm filter holders (eg VWR 402078401). A fluid tight seal was achieved using chemically resistant epoxy cement. See Supporting Information for further details of membrane mounting.

Effectiveness of the mounting method was confirmed by attaching a glass coverslip fragment in place of the carbon nanomembrane and verifying that no fluid flowed through the syringe filter even at a pressure of 100 kPa which was almost twice that used during any experimental run. In the case of water and ethanol, which required actual pressures >50 kPa to achieve flow rates >0.125 mL/min, observations at higher imposed flow rates were omitted and replaced by supplementary measurements at slower flows. The hazard that the fragile membrane might crack under hydraulic load was further mitigated by supporting the downstream side on a rigid metal grid with coarse apertures. It is important to note that this supporting mesh is likely to have restricted flow through immediately adjacent pores. The magnitude of this restriction was tested using a robust polycarbonate membrane with similar diameter pores (GE Osmonics, KN5CP01300, nominal 50 nm) to the carbon nanopipe arrays. Flow rates with the metal grid in place were observed to be 62.5 ± 7.7% lower than that without the supporting mesh. This observation is in close agreement with photoanalysis of the grid which estimates its porosity at 63 ± 1.5%. Since the behavior of the more brittle carbon nanopipe arrays may be different (and cannot be tested in the gridless state without fracturing), observed flow rates are reported both with and without making correction for reduced flow resulting from the supporting grid restriction.

The key variable measured during the experiment was the steady state pressure at a given rate of flow for a fluid through the carbon nanopipe array. The experimental setup is shown schematically in Figure 3. A syringe pump (Harvard Ap-

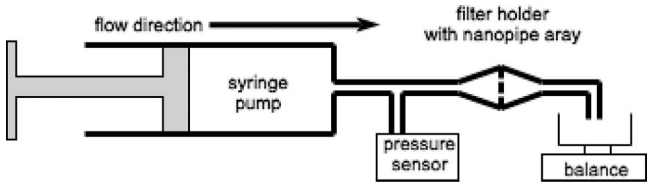

Figure 3. Schematic diagram of experimental setup. Fluid was driven by the syringe pump through the nanopipe array at a range of fixed rates. The stabilized pressure upstream of the membrane was measured for each flow state using a digital pressure meter. Fluid emerging from the nanopipe array was collected and periodically weighed to verify nominal flow rates.

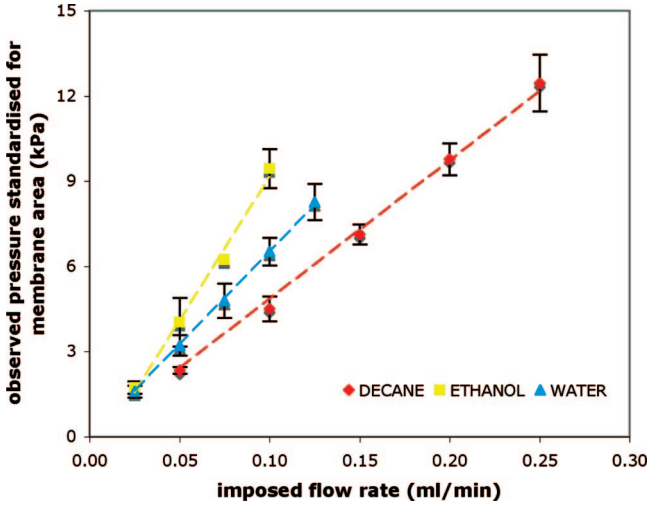

Figure 4. Plot of observed pressure against imposed flow rate for transport of three different fluids through an array of carbon nanopipes with pore size 43 ± 3 nm. Error bars show ±1 standard deviation for $n = 3$. At any given pressure, relative flow rate is fastest for decane and slowest for ethanol. As discussed in the main text, absolute pressure driven flow rates for all three fluids through the carbon nanopipes are considerably more than an order of magnitude faster than predicted by conventional theory.

paratus, Model 22 2400−01) with a 50 mL capacity glass syringe with Luer-Lok fitting was used to drive water, ethanol, and decane through the membrane mounted in a stainless steeel filter holder as previously described. 1.0 mm id PEEK tubing attached with fingertight and Luer-Lok PEEK fittings (Upchurch Scientific, part numbers 1538, P-656 and F-130X) was used to convey fluid between system components. A stainless steel pressure gauge tee (Upchurch Scientific, part number U-433) was located between the syringe pump and the filter holder to allow connection of a pressure sensor (Omega, PX-603−500G5V). Fluid pressure behind the membrane was monitored using a digital panel meter (Omega, DP25B−S-230) calibrated to kilopascals using a mercury manometer and reading 0 at 1 atm. PTFE tape was applied to the pressure sensor threads to ensure a tight seal.

Several further precautions were taken to ensure accurate measurements. All fluids were prefiltered through 20 nm pore size AAO membranes (Whatman, Anodisc 13) to exclude debris so as to minimize the possibility of channel blocking. Fluids were degassed under vacuum immediately prior to each experimental run, and the transport path was filled in a progressive manner so as to exclude air bubbles from the system. Fluid emerging from the carbon nanopipe array was periodically collected and weighed at timed intervals to verify the nominal flow rates set on the syringe pump. Pressure was recorded at each flow rate once readings in kilopascals were stable to one decimal place for a minimum continuous period of 60 s. All experiments took place at a consistent room temperature (23 ± 2 °C). Membrane integrity following flow measurements was verified by size exclusion of pressure driven 70 nm fluorescent labeled silica nanoparticles in aqueous solution (see Supporting Information).

A series of pressure measurements involving a minimum of three different carbon nanomembranes were obtained for each of the three fluids. The active area of each nanopipe array was determined from macrophotographs using automated pixel counting and the measured pressure corrected to a standard area of 1 cm^2. See Supporting Information for the detailed procedure.

Data from the experiment are presented in Figure 4. A positive linear relationship between pressure and flow rate was observed for water, decane, and ethanol with $R^2 > 0.99$ for a straight line fit in each case. The principal result is that the absolute flow rate for all three liquids through the 44 nm pore diameter carbon nanopipes is considerably more than an order of magnitude greater than predicted from conventional theory assuming Newtonian flow and following the Hagen−Poiseuille equation:

$$Q_0 = \frac{\pi R^4}{8\eta}\frac{\Delta p}{L} \quad (1)$$

where Q_0 is the volumetric flow rate, R is the inner nanopipe radius (22 nm), η is the dynamic viscosity of the fluid, Δp is the pressure drop, and L is the length of the pipe. The density of nanopipes crossing the membrane determined by analysis of SEM images was 1.07×10^{10} pores per cm^2, and the thickness of the membrane was 78 ± 2 μm (i.e., L). The viscosity of decane is 0.96 cP, and so for this fluid, the calculated flow rate for a pressure drop of 7.1 kPa through a single nanopipe should be 8.26×10^{-21} m^3 s^{-1}. The actual imposed flow rate across the whole membrane for this averaged pressure drop was 0.15 mL/min or 2.5×10^{-9} m^3 s^{-1}. The observed average flow rate of decane through a single nanopipe was therefore between 2.34×10^{-19} and 3.71×10^{-19} m^3 s^{-1}, depending on whether the assumption is made that the supporting metal grid effectively blocked flow through immediately adjacent pores. This implies a flow enhancement for decane through 44 nm diameter carbon nanopipes of 28 to 45 times. For ethanol, the enhancement factor was 16 to 25 times, and for water, it was 22 to 34 times. Enhanced flow (Q_E) is normally described using a slip length or coefficient l_s as in:

$$Q_E = Q_0\left(1 + \frac{4l_s}{R}\right) \quad (2)$$

The calculated slip coefficients and, for comparison, corresponding data from the cited recent studies of flow of the same fluids through smaller carbon nanotubes are set out in Table 1. A definition of slip coefficient and an explanation of its calculation is provided in the Supporting Information.

It is apparent from the results presented in Table 1 that the extent of flow enhancement observed for all fluids

Table 1. Summary of Flow Enhancement and Implied Slip Lengths Observed in the Present Study for Three Fluids through Carbon Nanopipes.[a] Corresponding Results from Two Recent Studies of Pressure Driven Flow through Smaller Carbon Nanotubes Are Provided for Comparison

	decane	ethanol	water
viscosity of fluid (Pa·s)	0.960	1.074	1.002
44 nm diameter nanopipes (this study)			
flow enhancement factor (ignoring effect of supporting grid)	28 ± 6	16 ± 1	22 ± 2
flow enhancement factor (allowing for effect of supporting grid)	45 ± 2	25 ± 2	34 ± 3
calculated slip length (nm, ignoring effect of supporting grid)	31 ± 2	21 ± 2	26 ± 2
calculated slip length (nm, allowing for effect of supporting grid)	41 ± 2	29 ± 2	35 ± 3
7 nm diameter nanotubes (Majumder et al. 2005)			
flow enhancement factor	3,941	32,143	61,404
calculated slip length (nm)	3,448	28,124	53,728
<2 nm diameter nanotubes (Holt et al. 2006)			
flow enhancement factor			560 to 8400
calculated slip length (nm)			140 to 1400

[a] Values are quoted ± 1 SD ($n = 3$) both with and without allowing for reduction of effective membrane area due to the supporting metal grid (see discussion in main text).

through ~44 nm carbon nanopipes is very much less than that reported in the previous studies through even smaller carbon pores. The measured enhancement nevertheless remains substantial at well over an order of magnitude and indicates that novel fluid flow phenomena occur to a significant extent even in the relatively large nanopipes used in this study. The flow rate at any given pressure through the 44 nm pores was greatest for decane, then for water, and slowest for ethanol. This relationship differs from that reported by Majumder et al. who found that water flowed fastest through their 7 nm nanotube channels, followed by ethanol with decane the slowest. In macroscale pipes ($d > 100\ \mu$m), where viscosity of the bulk fluid dominates, decane flows faster than water.[14] Majumder et al. attribute the relationship reversal they observed as being due to interaction between the water molecules and the hydrophobic carbon walls, with formation of a hydrogen bond network leading to very low friction. Our observation of greatest flow rate for decane suggests that at the length scale investigated (44 nm diameter pores) this effect is not significant.

The slip length of water observed in simulations of carbon nanotubes varies from ~10 nm[22] to plug flow[23] (infinite slip length) in 20,20 tubes. Plug flow was also seen in 16,16 tubes by Joseph and Aluru.[12] The predicted flow depends sensitively on the model pore, and fast flow will only be seen for accurate models of the graphene surface. Our experiments show fast flow for water in agreement with Majumder et al., Holt et al., and the majority of simulations. However, they differ as discussed above for ethanol and decane. The similarity between the flow of water and that of ethanol is not surprising given that they are both hydrogen bonded and presumably have similar behavior at carbon interfaces. Decane we know to have an extremely low friction coefficient on graphene. However, the surface of the nanopipe is not graphene but is thought to be amorphous, so the persistence of low friction is a mystery. This can be elucidated by molecular dynamics simulations of decane and water on amorphous carbon surfaces which are underway.

A full explanation for the significant flow enhancement observed in this and the previous cited studies is likely to be found in the precise structure of the pore wall and interactions between the molecules of the transported fluid and the inner carbon surface of the pore. In particular, the chemical character of this surface, including the presence of functional moieties such as H, OH, and COOH attached to the carbon network, is likely to influence behavior of the fluid. It is this surface interaction which becomes increasingly dominant as the pore diameter shrinks into the nanoscale regime causing the proportion of fluid molecules in immediate proximity to the carbon walls to increase relative to the number present in the bulk volume.

To characterize the chemical nature of the nanopipe surfaces, we have undertaken preliminary X-ray photon spectroscopy (XPS) analysis of carbon nanopipe arrays similar to those used in the work reported here. We have found evidence of light surface oxidation that is in accordance with previously reported observations[17] that these CVD produced pipes are less hydrophobic than the graphene walls of carbon nanotubes. We have investigated the relationship between surface functionalization of the nanopipes and the degree of flow enhancement for different fluids through them and will be reporting this work in a separate paper. This data will also assist our related work in developing accurate model surfaces for nanopipes.

Control of fluid interactions through surface modification promises to be an important technique for probing the novel physical processes underlying flow enhancement. It may also prove to be a useful tool in the fabrication of practical nanofluidic devices. Potential applications include water purification, materials separation, and the controlled transport of therapeutic agents across cell membranes. The confirmation of significantly enhanced flows in the larger and readily fabricated nanopipes reported here should facilitate the development of such applications exploiting this important new phenomenon.

Acknowledgment. N.Q. and M.W. acknowledge support from the EPSRC through Grant P09017 "Experimental Nanofluidics". M.W. acknowledges the support of the EPSRC through a doctoral training award, the Genetic Therapies Centre at Imperial College, and RGB Research Ltd for laboratory facilities. XPS analysis kindly provided by M.-L. Saboungi and R. Benoit at Centre de Recherche sur la Matière Divisée, CNRS, Orleans, France.

Supporting Information Available: Characterization of commercially available <100 nm AAO templates; method for production of AAO templates; appearance of AAO templates before and after CVD treatment; method for mounting nanopipe arrays in filter holder; method for determining active area of nanoipe arrays and standardizing observed pressures; method for verifying membrane integrity; Poiseuille flow and calculation of slip coefficient. This material is available free of charge via the Internet at http://pubs.acs.org.

References

(1) Whitby, M.; Quirke, N. *Nature Nanotechnology* **2007**, *2* (2), 87–94.
(2) Hinds, B. J. Aligned carbon nanotube membranes. In *Carbon Nanotechnoogy*, Dai, L., Ed. Elsevier B. V., 2006.
(3) Martin, C. R.; Kohli, P. *Nat. Rev. Drug Discovery* **2003**, *2* (1), 29–37.
(4) Srivastava, A.; Srivastava, O. N.; Talapatra, S.; Vajtai, R.; Ajayan, P. M. *Nat. Mater.* **2004**, *3* (9), 610–614.
(5) Dai, L. *Carbon Nanotechnology*. Elsevier, 2006.
(6) Gogotsi, Y. *Carbon Nanomaterials*. Taylor & Francis, 2006.
(7) Majumder, M.; Chopra, N.; Andrews, R.; Hinds, B. J. *Nature* **2005**, *438* (7064), 44–44.
(8) Holt, J. K.; Park, H. G.; Wang, Y. M.; Stadermann, M.; Artyukhin, A. B.; Grigoropoulos, C. P.; Noy, A.; Bakajin, O. *Science* **2006**, *312* (5776), 1034–1037.
(9) Skoulidas, A. I.; Ackerman, D. M.; Johnson, J. K.; Sholl, D. S. *Phys. Rev. Lett.* **2002**, *89* (18),
(10) Sokhan, V. P.; Nicholson, D.; Quirke, N. *J. Chem. Phys.* **2002**, *117* (18), 8531–8539.
(11) Supple, S.; Quirke, N. *Phys. Rev. Lett.* **2003**, *90* (21),
(12) Joseph, S.; Aluru, N. R. *Nano Lett.* **2008**,
(13) Pfahler, J.; Harley, J.; Bau, H.; Zemel, J. *Sensors and Actuators A-Physical* **1990**, *22* (1−3), 431–434.
(14) Cheng, J. T.; Giordano, N. *Phys. Rev. E* **2002**, *65* (3),
(15) Che, G.; Lakshmi, B. B.; Martin, C. R.; Fisher, E. R.; Ruoff, R. S. *Chem. Mater.* **1998**, *10* (1), 260–267.
(16) Martin, C. R. *Science* **1994**, *266* (5193), 1961–1966.
(17) Masuda, H.; Fukuda, K. *Science* **1995**, *268* (5216), 1466–1468.
(18) Nielsch, K.; Choi, J.; Schwirn, K.; Wehrspohn, R. B.; Gosele, U. *Nano Lett.* **2002**, *2* (7), 677–680.
(19) Rossi, M. P.; Ye, H. H.; Gogotsi, Y.; Babu, S.; Ndungu, P.; Bradley, J. C. *Nano Lett.* **2004**, *4* (5), 989–993.
(20) Supple, S.; Quirke, N. *J. Chem. Phys.* **2004**, *121* (17), 8571–8579.
(21) Supple, S.; Quirke, N. *J. Chem. Phys.* **2005**, *122* (10), 104706 1–6.
(22) Kotsalis, E. M.; Walther, J. H.; Koumoutsakos, P. *Int. J. Multiphase Flow* **2004**, *30* (7−8), 995–1010.
(23) Hanasaki, I.; Nakatani, A. *J. Chem. Phys.* **2006**, *124* (17),

NL080705F